World Journal of Engineering Research and Technology
WJERT
www.wjert.org
SJIF Impact Factor: 4.326

MODELLING HYDROMAGNETIC TURBULENT FREE CONVECTION FLUID FLOW OVER AN IMMERSED INFINITE VERTICAL CYLINDER

W. O. Mukuna[1]*, J. K. Kwanza[2], J. K. Sigey[2] and J. A. Okello[2]

[1]Department of Mathematics and Computer Science, University of Kabianga, P.O Box 2030 Kericho, 20200, Kenya.

[2]Department of Pure and Applied Mathematics, Jomo Kenyatta University of Agriculture and Technology, P. O. Box 62000 Nairobi, 00200, Kenya.

Article Received on 14/02/2017 Article Revised on 07/03/2017 Article Accepted on 27/03/2017

***Corresponding Author**
W. O. Mukuna
Department of Mathematics and Computer Science, University of Kabianga, P.O Box 2030 Kericho, 20200, Kenya.

ABSTRACT

A mathematical model of hydromagnetic turbulent boundary layer fluid flow past a vertical infinite cylinder with Hall current is considered. The fluid flows along the axis of the cylinder. The fluid flow is impulsively started and the flow problem is subsequently analysed. The flow is modeled using the momentum, energy and concentration conservation equations. The Reynolds stresses arising due to turbulence in the conservation equations are resolved using Prandtl mixing length hypothesis. The equations are then solved by a finite difference method. The effects of flow parameters on the primary velocity, secondary velocity, temperature and concentration profiles are investigated. The skin friction, rate of heat and mass transfer are computed and presented in tables. While the effect of Hall current on Primary velocity was not observed due to turbulence there was decreased secondary velocity profile when Hall parameter was increased.

KEY WORDS: Turbulent flow, Hall current, vertical cylinder, MHD flow, free convection, finite difference.

Nomenclature

Symbol	Quantity
j	current density, A/m^2
H	magnetic field intensity, Wb/m^2
H_0	constant magnetic field intensity, Wb/m^2
t	time, s
E	electric field, V/m
$U_r, \mathrm{U}_\theta, \mathrm{U}_\mathrm{x}$	components of velocity in the r, θ, and x axes respectively, m/s
P	pressure of the fluid, N/m^2
P_e	pressure of the fluid, N/m^2
T	absolute temperature, K
C_p	specific heat at constant pressure of the fluid, $J/kg/K$
D	characteristic diameter, m
r^*, θ^*, x^*	dimensional cylindrical coordinatesf the fluid,
ω_e	electron cyclotron frequency, Hz
t^*	dimensional time, s
T^*	dimensional temperature, K
T^*_∞	temperature of the fluid in the free stream, K
T^*_w	temperature of the fluid at the plate, K
U, V	dimensionless mean velocity components in θ and r axes respectively,
t	dimensionless time, s
Re	Reynolds number
M^2	magnetic parameter
m	Hall parameter
Pr	Prandtl number
Pr_t	turbulent Prandtl number
Sc	Schmidt number
Sc_t	turbulent Schmidt number

Greek symbols

Symbol	Quantity
ρ	fluid density, kg/m^3
μ	coefficient of viscosity, kg/ms
μ_0	magnetic permeability, H/m
$\Delta t, \Delta r$	time and distance intervals
ν	kinematic viscosity, m^2/s
τ_e	collision time of electron, s
θ	dimensionless fluid temperature
σ	electrical conductivity, $\Omega^{-1}m^{-1}$ s

INTRODUCTION

Research in fluid flow in the presence of magnetic field continues to attract increased interest from scientist and engineers. More particularly turbulent flows in the presence of magnetic field continue to attract more research attention as most practical fluid flows are turbulent. Verron J. and Sommeria J., (1987) carried out a numerical simulation of a two-dimensional turbulence experiment in magnetohydrodynamics. The setup consisted of a layer of mercury enclosed in a square box and driven by the injection of electric currents in a uniform magnetic field. They used a numerical finite difference model to simulate the Navier–Stokes equation in two dimensions with steady forcing and linear bottom friction.

Kim S. J. and Lee C. M.,(2002), carried out an investigation of the flow around a circular cylinder under the influence of an electromagnetic force. In their investigation, the effect of the local electromagnetic body force on the flow behavior around a circular cylinder was conducted.

Kinyanjui et al (2012) presented their work on hydromagnetic turbulent flow of rotating system past a semi-infinite vertical plate with Hall current. Kwanza et al, (2010) presented a study on a mathematical model of turbulent convective fluid flow past a vertical infinite plate with Hall current. They investigated a magnetohydrodynamics (MHD) turbulent boundary layer fluid flow past a vertical infinite plate in a dissipative fluid with Hall current. They used Prandtl mixing length hypothesis to resolve turbulence stress terms in the momentum equation. They concluded that increase in Hall parameter led to increase in velocity profiles.

Benim et al (2008) modelled turbulent flow past a circular cylinder by RANS, URANS, LES and DES.

Yoon et al (2004) carried out a numerical study on the fluid flow and heat transfer around a circular cylinder in an aligned magnetic field. In the study they numerically investigated two-dimensional laminar fluid flow and heat transfer past a circular cylinder in an aligned magnetic field using the spectral method. They concluded that as the intensity of applied magnetic fields increases, the vortex shedding formed in the wake becomes weaker and the oscillating amplitude of lift coefficient decreases. Takhar et al (2000) studied combined heat and mass transfer along a vertical moving cylinder with a free stream. Datta et al (2006) investigated the effect of non-uniform slot injection (suction) on a forced flow over a slender cylinder.

Sarris et al (2010) presented their work on Magnetic field effect on the cooling of a low-Pr fluid in a vertical cylinder. In their work they carried out direct numerical simulations for the transient and turbulent natural convection cooling of an initially isothermal quiescent liquid metal placed in a vertical cylinder in the presence of a vertical magnetic field. The numerical results showed that the magnetic field had no observable effect at the initial stage of the vertical boundary layer development and conduction heat transfer was favored during the transition stage. Singh et al (2008) presented their work on unsteady mixed convection from a rotating vertical slender cylinder in an axial flow.

Ahmet Kaya (2011) presented a study on heat and mass transfer from a horizontal slender cylinder with a magnetic field effect. In the study a uniform magnetic field was applied perpendicular to the cylinder. The nonlinear partial differential equations governing the flow were transformed into similar boundary layer equations, which were then solved numerically. The transverse curvature parameter, the magnetic parameter, the Prandtl number and the Schmidt number were the main parameters. He concluded that the local skin friction coefficient, the local heat transfer coefficient and the local mass transfer coefficient increase with an increase in the magnetic parameter and transverse curvature parameter.

In the current investigation a study is carried out on turbulent fluid flow over an infinite vertical infinite cylinder in the presence of a strong magnetic field.

Mathematical model

We consider a two dimensional turbulent boundary layer flow. The fluid flow is along a vertical infinitely long cylinder lying in the x-y plane. The cylinder is immersed in the fluid. The axis of the cylinder is in the positive x-axis direction and the fluid flows upwards positive x-axis direction parallel to the axis of the cylinder. The cylinder is assumed to have non-end effects. The fluid is assumed incompressible and viscous. A strong magnetic field of uniform strength H_0 is applied along the x-axis. The induced magnetic field is considered negligible hence H = (0, 0, H_0). The temperature of the surface of the cylinder and the fluid are assumed to be the same initially. At time $t^*>0$ the fluid starts moving impulsively with velocity U_0 and at the same time the temperature of the cylinder is instantaneously raised to T_W^* which is maintained constant later on. Given that the flow is over a cylinder, cylindrical coordinate form of the governing equations are used. The flow is considered to be along the axial and angular components. There is no radial flow. Thus the two dimensions of this flow are x and θ.

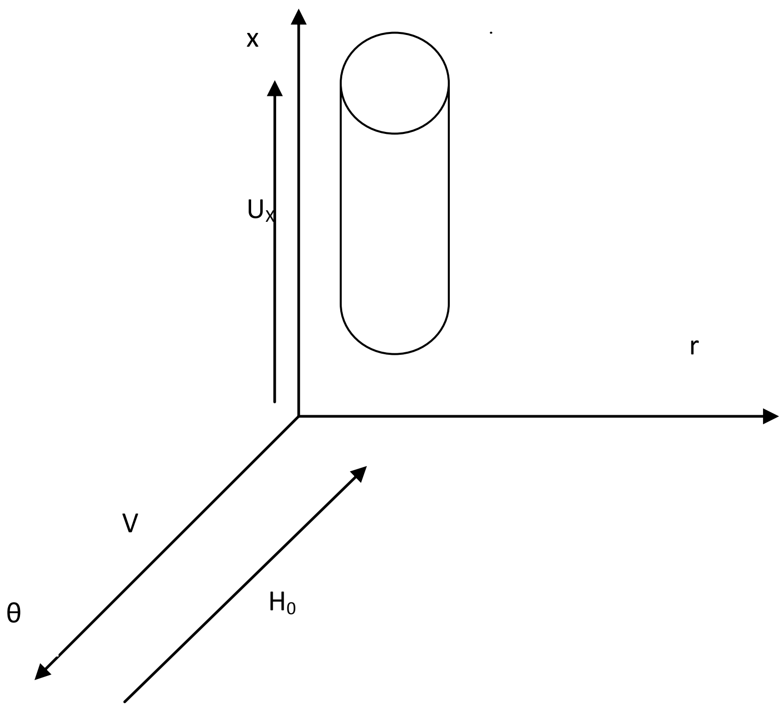

Figure 1: Schematic diagram of the problem.

The above flow is governed by the following cylindrical coordinate equations:

$$\frac{\partial \overline{U}_x}{\partial t} = -\frac{1}{\rho}\frac{\partial \overline{P}}{\partial x} + \nu\left(\frac{\partial^2 U_x}{\partial r^2} + \frac{1}{r}\frac{\partial U_x}{\partial r}\right) - \left[\frac{1}{r}\frac{\partial \overline{U'_x U'_r}}{\partial r}\right] + \rho g + \vec{J} \times B\Big|_x \quad (1)$$

$$\frac{\partial\overline{U_\theta^*}}{\partial t^*}=\nu\left(\frac{\partial^2\overline{U_\theta^*}}{\partial r^{*2}}+\frac{1}{r^*}\frac{\partial\overline{U_\theta^*}}{\partial r^*}-\frac{\overline{U_\theta^*}}{r^{*2}}\right)-\left[\frac{\partial\overline{U_r'U_\theta'}}{\partial r^*}-\frac{2\overline{U_\theta'U_r'}}{r^*}\right]+\vec{J}\times B\Big|_\theta \quad (2)$$

$$\rho C_p\left(\frac{\partial\overline{T^*}}{\partial t^*}\right)=k\left(\frac{\partial^2\overline{T^*}}{\partial r^{*2}}+\frac{1}{r*}\frac{\partial\overline{T^*}}{\partial r^*}\right)-\ \rho C_p\left(\frac{\partial(\overline{U_r'T'})}{\partial r^*}\right) \quad (3)$$

$$\left(\frac{\partial\overline{C^*}}{\partial t^*}\right)=D\left(\frac{\partial^2\overline{C^*}}{\partial r^{*2}}+\frac{1}{r^*}\frac{\partial\overline{C^*}}{\partial r^*}\right)-\left(\frac{\partial(\overline{U_r'C'})}{\partial r}\right) \quad (4)$$

The boundary and initial conditions are:

$t^*<0:U_x{}^*=0,U_\theta{}^*=0,T^*=T_\infty^*,C=C_\infty^*$ everywhere (5a)

$t^*\geq 0:U_x{}^*=U_0,U_\theta{}^*=0,T^*=T_W^*,C=C_W^*$ at $r^*=\frac{D}{2}$ (D is the diameter of the cylinder.) (5b)

$U_x{}^*\to 0,U_\theta{}^*\to 0,T^*\to T_\infty^*,C\to C_\infty^*$ as $r^*\to\infty$ (5c)

The pressure gradient in the x-axis direction results from the change in elevation up the cylinder. Thus:

$$\frac{\partial P}{\partial x}=-\rho_\infty g$$

Hence equation (1) becomes:

$$\rho\frac{\partial\overline{U}_x}{\partial t}=(\rho_\infty-\rho)g+\mu\left(\frac{\partial^2U_x}{\partial r^2}+\frac{1}{r}\frac{\partial U_x}{\partial r}\right)-\rho\left[\frac{1}{r}\frac{\partial\overline{U_x'U'_r}}{\partial r}\right]+\vec{J}\times B\Big|_x \quad (6)$$

The density difference ρ- ρ∞ may be expressed in terms of the volume coefficient of expansion β defined by Holman (2010) as: $\beta=\frac{1}{V}\left(\frac{\partial V}{\partial T}\right)_P=\frac{1}{V_\infty}\cdot\frac{V-V_\infty}{T-T_\infty}=\frac{\rho_\infty-\rho}{\rho(T-T_\infty)}$ (7)

Such that (6) becomes

$$\rho\frac{\partial\overline{U}_x}{\partial t}=\rho\beta g(T-T_\infty)+\mu\left(\frac{\partial^2U_x}{\partial r^2}+\frac{1}{r}\frac{\partial U_x}{\partial r}\right)-\rho\left[\frac{1}{r}\frac{\partial\overline{U_x'U'_r}}{\partial r}\right]+\vec{J}\times B\Big|_x \quad (8)$$

Which simplifies to

$$\frac{\partial\overline{U}_x}{\partial t}=\beta g(T-T_\infty)+\nu\left(\frac{\partial^2U_x}{\partial r^2}+\frac{1}{r}\frac{\partial U_x}{\partial r}\right)-\left[\frac{1}{r}\frac{\partial\overline{U_x'U'_r}}{\partial r}\right]+\vec{J}\times B\Big|_x \quad (9)$$

Taking into account the mass flow and considering the analogy between heat and mass and using (*) to indicate dimension, equation (8) becomes.

$$\frac{\partial \overline{U_x^*}}{\partial t^*} = \beta g\left(T^* - T_\infty^*\right) + \nu\left(\frac{\partial^2 \overline{U_{x\,x}^*}}{\partial r^{*2}} + \frac{1}{r^*}\frac{\partial \overline{U_x^*}}{\partial r^*}\right) - \left[\frac{1}{r^*}\frac{\partial \overline{U_x' U_r'}}{\partial r^*}\right] + \beta^{"} g\left(C^* - C_\infty^*\right) + \vec{J}\times B\big|_x \qquad (9)$$

Next, we seek to establish the components of the electromagnetic force term in 4.9 and 4.2 that is the term: $\vec{J}\times\vec{B}$

The equation of conservation of charge $\nabla .J = 0$, gives $j_r = k$, a constant, where $\vec{J} = (j_r, j_\theta, j_z)$. The constant is zero since, $j_r = 0$ at the cylinder which is insulated. Thus $j_r = 0$ everywhere in the flow. Neglecting the ion-slip and thermoelectric effects, generalized Ohm's law including the effects of Hall current gives (Cowling (1957))

$$\vec{J} + \frac{w_e\tau_e}{H_0}(\vec{J}\times\vec{H}) = \sigma\left(\vec{E} + \mu_0\vec{q}\times\vec{H} + \frac{1}{en_e}\nabla P_e\right) \qquad (10)$$

For the problem we seek to solve there is no applied electric field hence $\vec{E} = 0$ and thus neglecting electron pressure, equation (10) becomes

$$\vec{J} + \frac{w_e\tau_e}{H_0}(\vec{J}\times\vec{H}) = \sigma\mu_0\left(\vec{q}\times\vec{H}\right) \qquad (11)$$

Given that $\vec{H} = (0,0,H_0)$ and taking $\vec{J} = \left(0, j_{\theta,} j_x\right)$, $\vec{q} = \left(0, U_\theta, U_x\right)$ and $\vec{B} = \mu_0\vec{H}$ simplifying equation (11) and solving gives:

$$j_r = 0 \qquad (12a)$$

$$j_\theta = \frac{\sigma\mu_0 H_0(U_z + mU_\theta)}{1+m^2} \qquad (12b)$$

$$j_z = \frac{\sigma\mu_0 H_0(mU_z - U_\theta)}{1+m^2} \qquad (12c)$$

Where $m = w_e\tau_e$ is the Hall parameter.

Thus the electromagnetic force along θ and x-axis from (12) are respectively:

$$\left(J\times B\right)_\theta = \frac{\sigma\mu_0^2 H_0^2(mU_z - U_\theta)}{1+m^2} \qquad (13a)$$

$$\left(J\times B\right)_x = \frac{-\sigma\mu_0^2 H_0^2(U_z + mU_\theta)}{1+m^2} \qquad (13b)$$

Hence the governing equations (9) and (2) are respectively:

$$\frac{\partial \overline{U_x^*}}{\partial t^*} = \nu\left(\frac{\partial^2 \overline{U_{xx}^*}}{\partial r^{*2}} + \frac{1}{r^*}\frac{\partial \overline{U_x^*}}{\partial r^*}\right) - \left[\frac{1}{r^*}\frac{\partial \overline{U'_x U'_r}}{\partial r^*}\right] + \beta'' g\left(C^* - C_\infty^*\right) + \beta g\left(T^* - T_\infty^*\right) - \frac{\sigma\mu_0^2 H_0^2(\overline{U_x^*} + m\overline{U_\theta^*})}{1+m^2} \tag{14}$$

$$\frac{\partial \overline{U_\theta^*}}{\partial t^*} = \nu\left(\frac{\partial^2 \overline{U_\theta^*}}{\partial r^{*2}} + \frac{1}{r^*}\frac{\partial \overline{U_\theta^*}}{\partial r^*} - \frac{\overline{U_\theta^*}}{r^{*2}}\right) - \left[\frac{\partial \overline{U'_r U'_\theta}}{\partial r^*} - \frac{2\overline{U'_\theta U'_r}}{r^*}\right] + \frac{\sigma\mu_0^2 H_0^2(m\overline{U_x^*} - \overline{U_\theta^*})}{1+m^2} \tag{15}$$

Non-dimensionalization

To non-dimensionalize equations (3), (4), (14) and (15), the following scaling variables are applied in the non-dimensionalization process:

$$t = \frac{t^* U_0^2}{\nu}; r = \frac{r^* U_0}{\nu}; U_i = \frac{U_i^*}{U_0}; \theta = \frac{T^* - T_\infty^*}{T_w^* - T_\infty^*} \quad C = \frac{C^* - C_\infty^*}{C_w^* - C_\infty^*} \tag{16a, b, c, d, e}$$

The (*) superscript denotes the dimensional variables, Uo is the reference velocity, r is the radius of the cylinder, T^*_w - T^*_∞ is the temperature difference between the surface and the free stream temperature and C^*_w - C^*_∞ is the mass difference between the surface and the free stream .

The transformation gives:

$$\frac{\partial U_x}{\partial t} = \left(\frac{\partial^2 U_x}{\partial r^2} + \frac{1}{r}\frac{\partial U_x}{\partial r}\right) - \left[\frac{1}{r}\frac{\partial \overline{U'_x U'_r}}{\partial r}\right] + Gr\theta + Gr_m C - M^2\frac{(U_x + mU_\theta)}{\left(1+m^2\right)} \tag{17}$$

$$\frac{\partial U_\theta}{\partial t} = \left(\frac{\partial^2 U_\theta}{\partial r^2} + \frac{1}{r}\frac{\partial U_\theta}{\partial r} - \frac{U_\theta}{r^2}\right) - \left[\frac{\partial \overline{U'_x U'_r}}{\partial r} - \frac{2\overline{U'_\theta U'_r}}{r}\right] + M^2\frac{(mU_x - U_\theta)}{\left(1+m^2\right)} \tag{18}$$

$$\frac{\partial \theta}{\partial t} = \frac{1}{\Pr}\left(\frac{\partial^2 \theta}{\partial r^2} + \frac{1}{r}\frac{\partial \theta}{\partial r}\right) - \frac{\partial(\overline{U''_r \theta'})}{\partial r} \tag{19}$$

$$\left(\frac{\partial C}{\partial t}\right) = \frac{1}{Sc}\left(\frac{\partial^2 C}{\partial r^2} + \frac{1}{r}\frac{\partial C}{\partial r}\right) - \left(\frac{\partial(\overline{U'_r C'})}{\partial r}\right) \tag{20}$$

Where:

$$Gr = \nu g\beta\frac{T_w^* - T_\infty^*}{U_0^3}$$

$$Gr_m = \nu g\beta\frac{C_w^* - C_\infty^*}{U_0^3}$$

$$Sc = \frac{\nu}{D}$$

Pr = μC$_p$/k

$$M^2 = \frac{\sigma \mu_0^2 H_0^2 \nu}{U_0^2}.$$

Boundary and initial conditions

The non-dimensional form of (5) becomes:

$$t < 0 : U_x = 0, U_\theta = 0, \theta = 0, C = 0 \text{ everywhere} \tag{21a}$$

$$t \geq 0 : U_x = 1, U_\theta = 0, \theta = 1, C = 1 \text{ at } r = \frac{1}{2} \tag{21b}$$

$$U_x \to 0, U_\theta \to 0, \theta \to 0, C \to 0 \text{ as } r \to \infty \tag{21c}$$

Resolving turbulence stresses

Applying Prandtl mixing length hypothesis as in [4] equations (17) - (20) simplifies to:

$$\frac{\partial U_x}{\partial t} = \left(\frac{\partial^2 U_x}{\partial r^2} + \frac{1}{r}\frac{\partial U_x}{\partial r} \right) + k^2 r \left(\frac{\partial U_x}{\partial r} \right)\left(\frac{\partial U_x}{\partial r} \right) + Gr\theta + Gr_m C - M^2 \frac{(U_x + mU_\theta)}{(1+m^2)} \tag{22}$$

$$\frac{\partial U_\theta}{\partial t} = \left(\frac{\partial^2 U_\theta}{\partial r^2} + \frac{1}{r}\frac{\partial U_\theta}{\partial r} - \frac{U_\theta}{r^2} \right) + 2k^2 r^2 \left(\frac{\partial U_\theta}{\partial r} \right)\left(\frac{\partial^2 U_\theta}{\partial r^2} \right) + M^2 \frac{(mU_x - U_\theta)}{(1+m^2)} \tag{23}$$

$$\frac{\partial \theta}{\partial t} = \frac{1}{\Pr}\left(\frac{\partial^2 \theta}{\partial r^2} + \frac{1}{r}\frac{\partial \theta}{\partial r} \right) + \frac{k^2 r^2}{\Pr_t}\left(\frac{\partial U_x}{\partial r} \right)\left(\frac{\partial \theta}{\partial r} \right) \tag{24}$$

$$\left(\frac{\partial C}{\partial t} \right) = \frac{1}{Sc}\left(\frac{\partial^2 C}{\partial r^2} + \frac{1}{r}\frac{\partial C}{\partial r} \right) + \frac{k^2 r^2}{Sc_t}\left(\frac{\partial U_x}{\partial r} \right)\left(\frac{\partial C}{\partial r} \right) \tag{25}$$

Finite Difference Scheme

Considering that the systems of partial differential equations we seek to solve are highly non-linear their analytic solutions are not possible. We thus approximate their solutions by finite difference method. In the following finite difference scheme the primary velocity U_x is denoted by U and the secondary velocity U_θ is denoted by V to reduce the subscripts as we use i and j as subscripts, i corresponding to r as j corresponds to t. The equivalent finite difference scheme for equations (22)-(25) are respectively:

$$U_{(i,j+1)} = U_{(i,j)} + \Delta t \left(\frac{U_{(i+1,j)} - 2U_{(i,j)} + U_{(i-1,j)}}{(\Delta r)^2} + \frac{1}{i\Delta r}\frac{U_{(i+1,j)} - U_{(i,j)}}{\Delta r} \right) +$$

$$k^2 i(\Delta r)(\Delta t)\left(\frac{U_{(i+1,j)} - U_{(i,j)}}{\Delta r}\right)^2 + \Delta t\{\ Gr\theta_{(i,j)} + Gr_m C_{(i,j)} - M^2 \frac{(U_{(i,j)} + mV_{(i,j)})}{1+m^2}\ \} \quad (26)$$

$$V_{(i,j+1)} = V_{(i,j)} + \Delta t\left(\frac{V_{(i+1,j)} - 2V_{(i,j)} + V_{(i-1,j)}}{(\Delta r)^2} + \frac{1}{i\Delta r}\frac{V_{(i+1,j)} - V_{(i,j)}}{\Delta r} - \frac{V_{(i,j)}}{(i\Delta r)^2}\right) +$$

$$2k^2 (i\Delta r)^2 (\Delta t)\left(\frac{V_{(i+1,j)} - V_{(i,j)}}{\Delta r}\right)\left(\frac{V_{(i+1,j)} - 2V_{(i,j)} + V_{(i-1,j)}}{(\Delta r)^2}\right) + \Delta t M^2 \frac{(mU_{(i,j)} - V_{(i,j)})}{1+m^2} \quad (27)$$

$$\theta_{(i,j+1)} = \theta_{(i,j)} + \frac{\Delta t}{\Pr}\left(\frac{\theta_{(i+1,j)} - 2\theta_{(i,j)} + \theta_{(i-1,j)}}{(\Delta r)^2} + \frac{1}{i\Delta r}\frac{\theta_{(i+1,j)} - \theta_{(i,j)}}{\Delta r}\right) +$$

$$\frac{k^2 (\Delta t)(i\Delta r)^2}{\Pr_t}\left(\frac{U_{(i+1,j)} - U_{(i,j)}}{\Delta r}\right)\left(\frac{\theta_{(i+1,j)} - \theta_{(i,j)}}{\Delta r}\right) \quad (28)$$

$$C_{(i,j+1)} = C_{(i,j)} + \frac{\Delta t}{Sc}\left(\frac{C_{(i+1,j)} - 2C_{(i,j)} + C_{(i-1,j)}}{(\Delta r)^2} + \frac{1}{i\Delta r}\frac{C_{(i+1,j)} - C_{(i,j)}}{\Delta r}\right) +$$

$$\frac{k^2 (\Delta t)(i\Delta r)^2}{Sc_t}\left(\frac{U_{(i+1,j)} - U_{(i,j)}}{\Delta r}\right)\left(\frac{C_{(i+1,j)} - C_{(i,j)}}{\Delta r}\right) \quad (29)$$

Where i and j refer to r and t respectively. r have been substituted with $i\Delta r$.

The boundary and initial conditions take the form:

$$j < 0 : U_{(i,j)} = 0, V_{(i,j)} = 0, \theta_{(i,j)} = 0, C_{(i,j)} = 0 \text{ everywhere} \quad (30a)$$

$$j \geq 0 : U_{(i,j)} = 1, V(i,j) = 0, \theta_{(i,j)} = 1, C_{(i,j)} = 1 \text{ at } i = \frac{\text{Re}}{2} \quad (30b)$$

$$U_{(i,j)} \to 0, V_{(i,j)} \to 0, \theta_{(i,j)} \to 0, C_{(i,j)} \to 0 \text{ as } i \to \infty \quad (30c)$$

The solution was computed and the results displayed in graphs and tables as shown in figures 2 to 5 and tables 1 - 3.

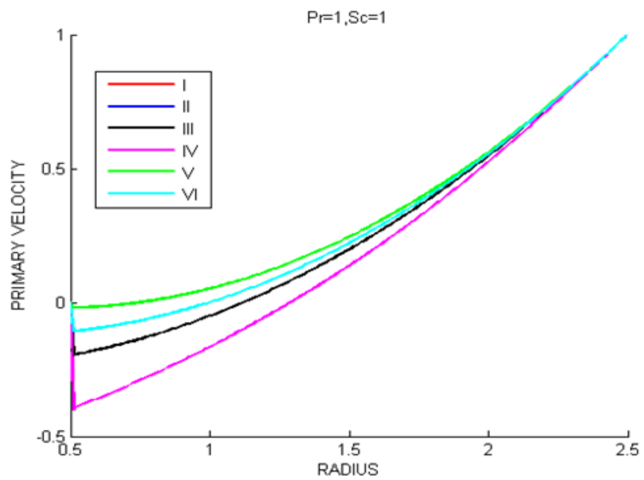

	M^2	m	t	Gr	Grm
I	2	2	0.2	-1.0E4	-1.0E4
II	4	2	0.2	-1.0E4	-1.0E4
III	2	4	0.2	-1.0E4	-1.0E4
IV	2	2	0.4	-1.0E4	-1.0E4
V	2	2	0.2	-1.0E3	-1.0E4
VI	2	2	0.2	-1.0E4	-1.0E3

Figure 2: Primary velocity profiles with heating of the cylinder.

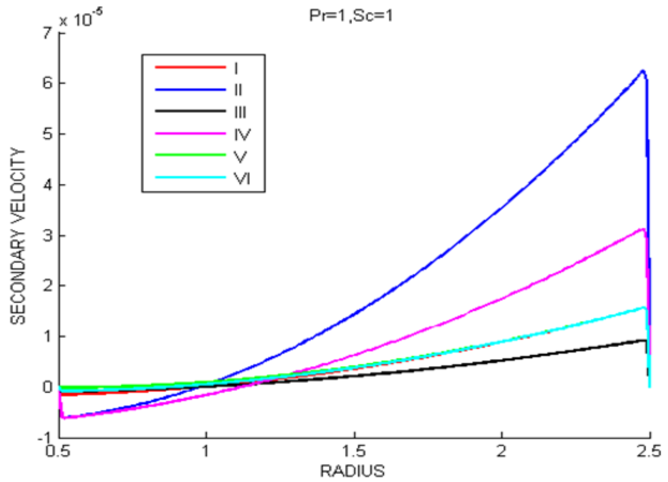

	M^2	m	t	Gr	Grm
I	2	2	0.2	-1.0E4	-1.0E4
II	4	2	0.2	-1.0E4	-1.0E4
III	2	4	0.2	-1.0E4	-1.0E4
IV	2	2	0.4	-1.0E4	-1.0E4
V	2	2	0.2	-1.0E3	-1.0E4
VI	2	2	0.2	-1.0E4	-1.0E3

Figure 3: Secondary velocity profiles with heating of the cylinder.

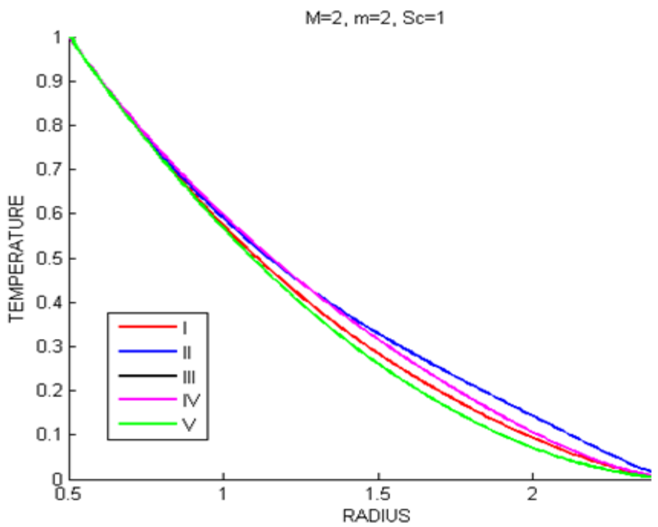

	t	Gr	Grm	Pr
I	0.2	-1.0E4	-1.0E4	1
II	0.4	-1.0E4	-1.0E4	1
III	0.2	-2.0E5	-1.0E4	1
IV	0.4	-1.0E4	-2.0E5	1
V	0.2	-1.0E3	-1.0E4	10

Figure 4: Temperature profiles with heating of the cylinder.

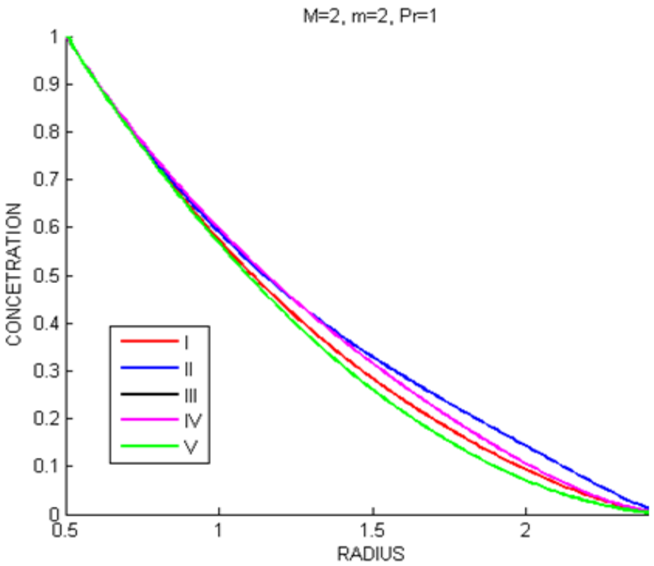

	t	Gr	Grm	Sc
I	0.2	-1.0E4	-1.0E4	1
II	0.4	-1.0E4	-1.0E4	1
III	0.2	-2.0E5	-1.0E4	1
IV	0.4	-1.0E4	-2.0E5	1
V	0.2	-1.0E3	-1.0E4	10

Figure 5: Concentration profiles with heating of the cylinder.

Table 1: Skin friction values for heating of the cylinder.

	M^2	m	t	Gr	Grm	τ_u	τ_v
I	2	2	0.2	-1.0E4	-1.0E4	0.0033	-2.6353E-7
II	4	2	0.2	-1.0E4	-1.0E4	0.0033	-1.05411E-6
III	2	4	0.2	-1.0E4	-1.0E4	0.0033	-1.5501E-7
IV	2	2	0.4	-1.0E4	-1.0E4	0.0033	-2.6353E-7
V	2	2	0.2	-1.0E3	-1.0E4	0.00033	-2.6341E-7
VI	2	2	0.2	-1.0E4	-1.0E3	0.0018	-2.6347E-7

Table 2: Heat transfer values for heating of the cylinder.

	t	Gr	Grm	Pr	Nu
I	0.2	-1.0E4	-1.0E4	1	-7.6005E-4
II	0.4	-1.0E4	-1.0E4	1	-7.6005E-4
III	0.2	-2.0E5	-1.0E4	1	-7.5641E-4
IV	0.4	-1.0E4	-2.0E5	1	-7.5641E-4
V	0.2	-1.0E3	-1.0E4	10	-2.4066E-4

Table 3: Mass transfer values for heating of the cylinder.

	t	Gr	Grm	Sc	Sh
I	0.2	-1.0E4	-1.0E4	1	-7.6005E-4
II	0.4	-1.0E4	-1.0E4	1	-7.6005E-4
III	0.2	-2.0E5	-1.0E4	1	-7.5641E-4
IV	0.4	-1.0E4	-2.0E5	1	-7.5641E-4
V	0.2	-1.0E3	-1.0E4	10	-2.4066E-4

Determination of skin friction, the rate of heat transfer and the rate of mass transfer

Skin friction, the rate of heat transfer and the rate of mass transfer are determined from the velocity, temperature and concentration profiles. The rate of heat and mass transfer are given by $Nu = -\left.\frac{\partial \theta}{\partial r}\right|_{r=0.5}$ and $Sh = -\left.\frac{\partial C}{\partial r}\right|_{r=0.5}$ respectively.

The skin friction is given by, Rathy (1976),

$$\tau_u = -\left.\frac{\partial U}{\partial r}\right|_{r=0.5} \text{ and } \tau_v = -\left.\frac{\partial V}{\partial r}\right|_{r=0} \text{ where } \tau = \frac{\tau^*}{\rho U^2}$$

The above are calculated by numerical differentiation using Newton's interpolation formula over the first five points.

$$\tau_x = \frac{5}{6}\left[25u(0,i) - 48u(1,i) + 36u(2,i) - 16u(3,i) + 3u(4,i)\right] \quad (31)$$

$$\tau_y = \frac{5}{6}\left[25v(0,i) - 48v(1,i) + 36v(2,i) - 16v(3,i) + 3v(4,i)\right] \quad (32)$$

$$Nu = \frac{5}{6}\left[25\theta(0,i) - 48\theta(1,i) + 36\theta(2,i) - 16\theta(3,i) + 3\theta(4,i)\right] \quad (33)$$

$$Sh = \frac{5}{6}\left[25C(0,i) - 48C(1,i) + 36C(2,i) - 16C(3,i) + 3C(4,i)\right] \quad (34)$$

Analysis of results

The flow was considered when the cylinder is at a lower temperature than the surrounding leading to heating of the cylinder by free convection currents. Computationally this condition is satisfied by keeping the Grashof number less than zero. Because the flow being considered is turbulent the Grashof number is kept in the order of $-1\text{x}10^4$.

Primary velocity profiles

From figure 2 it is noted that:

(i) Primary velocity is not affected by magnetic parameter and Hall parameter.

(ii) There is a decrease in primary velocity profiles when Grashof number, modified Grashof number are increased.

(iii) An increase in time parameter leads to an increase in the primary velocity profiles.

Secondary velocity profiles

From figure 3 it is noted that:

(i) The secondary velocity profiles increase in magnitude with increase in time.

(ii) Secondary velocity profiles decrease with increase in Hall.

(iii) Increase in magnetic parameters leads to increase in secondary velocity profiles.

(iv) There is no significant change in the secondary velocity profiles with change in Grashof and Modified Grashof numbers.

Temperature profiles

From figure 4 it is noted that:

(i) There is no observable variation in temperature profiles with variation in magnetic parameter, Hall parameter and Schmidt numbers.

(ii) There is increase in temperature profiles with increase in Grashof number, modified Grashof number and time parameter.

(iii) There is decrease in temperature profiles with increase in Prandtl number.

Concentration profiles

From figure 5 it is noted that:

(i) There is increase in concentration profiles with increase in time parameter.

(ii) There is decrease in concentration profiles with increase in Grashof number, modified Grashof number and Schmidt number.

(iii) There is no observable variation in concentration profiles with variation in magnetic parameter, Hall parameter and Prandtl number.

Skin friction

From table 1 we observe that:

i) A variation in magnetic, Hall and time parameters does not affect the primary velocity skin friction.

ii) A decrease in both Grashof number and modified Grashof number leads to a decrease in primary velocity skin friction.

iii) An increase in Magnetic and Hall parameters leads to an increase in secondary velocity skin friction.

iv) Increase in time does not affect secondary velocity skin friction.

v) Decrease in both Grashof number and modified Grashof number leads to a decrease in secondary velocity skin friction

Heat transfer

From table 2 we observe that:

i) Change in time does not affect the rate of heat transfer.

ii) Increase in both Grashof number and modified Grashof number leads to a decrease in heat transfer.

iii) Increase in Prandtl number leads to an increase in heat transfer.

Mass transfer

From table 3 we observe that:

i) Change in time does not affect the rate of mass transfer.

ii) Increase in both Grashof number and modified Grashof number leads to a decrease in mass transfer.

iii) Increase in Schmidt number leads to an increase in mass transfer.

CONCLUSION

The hydromagnetic turbulent free convection flow of a conducting fluid over a vertical infinite cylinder is numerically investigated. The effects of various flow parameters on the mean velocity, mean temperature, skin friction and Nusselt and Sherwood numbers were obtained. The results can be summarized as follows:

i) The effect of Hall current on primary velocity is suppressed by turbulence. An increase in Hall parameter decreases secondary velocity while an increase in magnetic parameter increases secondary velocity profiles.

ii) It is observed that change in Hall parameter has no effect on temperature and concentration.

iii) Temperature and concentration profiles increases with increase in Grashof number and modified Grashof number respectively.

iv) There is decrease in temperature and concentration profiles with increase in Prandtl number and Schmidt number respectively.

v) A decrease in both Grashof number and modified Grashof number reduces both the primary and secondary skin friction

vi) Increase in Grashof number leads to a decrease in rate of heat and rate of mass transfers.

vii) Increase in Prandtl number and Schmidt number leads to increase in heat and mass transfer rates respectively.

This results are found to be consistent with previous results, for example Sarris et al.[9]

REFERENCES

1. Ahmet Kaya (2011) *Heat and mass transfer from a horizontal slender cylinder with a magnetic field effect* J. Of Thermal Science and Technology, 2011; 31(2): 73-78.
2. Benim A.C., Pasqualotto E., Suh S.H.; (2008) *Modelling turbulent flow past a circular cylinder by RANS, URANS, LES and DES.;* International Journal of Computational Fluid Dynamics, Volume 8, Number 5/2008; pp 299-307.
3. Cowling T.G., 1957; *Magnetohydrodynamics* New York: Interscience, 1957.
4. Datta P., Anilkumar, D., Roy, S. and Mahanti, N.C.,(2006) *Effect of non-uniform slot injection (suction) on a forced flow over a slender cylinder, Int. J. Heat Mass Transf,* 2006; 49: 2366-2371.
5. Holman, J. P., (2010) *Heat transfer —10th ed*. Mcgraw-Hill series in mechanical engineering.
6. Kim S. J. and Lee C. M., (2002), *Numerical Investigation of cross flow around a circular cylinder at a low Reynolds number flow under an electromagnetic force.* KSME International journal, Vol. 16 No. 3 pp 363 – 375.
7. Kinyanjui M., Emmah M., Jackson K. (2012). *Hydromagnetic turbulence flow of rotating system past a semi-infinite vertical plate with hall current*. International Journal of pure and Applied mathematics, Vol. 79, No. 1 97-119.
8. Kwanza J.K.; Mukuna W. O. and Kinyanjui M (2010).; *A mathematical model of turbulent convective fluid flow past a vertical infinite plate with Hall current;* International Journal of Modelling and Simulation, Vol. 30, No. 3, pg 376- 386.
9. Sarris E., Iatridis A. I., Dritselis C. D., and Vlachos N. S., (2010); *Magnetic field effect on the cooling of a low-Pr fluid in a vertical cylinder*; Physics of Fluids, 22: 017101.
10. Singh, P.J., Roy, S. and Pop I., (2008) *Unsteady mixed convection from a rotating vertical slender cylinder in an axial flow,* Int. J. Heat Mass Transf, 51: 1423-1430.
11. Takhar, H.S., Chamkha, A.J. and Nath, G., (2000) *Combined heat and mass transfer along a vertical moving cylinder with a free stream, Heat Mass Transf*. 36: 237-246.
12. Verron J. and Sommeria J., (1987). *"Numerical simulation of a two-dimensional turbulence experiment in magnetohydrodynamics,"* Physics of Fluids, Vol. 30, pp 732-747.
13. Yoon H. S., Chun H. H., Ha M. Y., and Lee H. G., (2004) "*A numerical study on the fluid flow and heat transfer around a circular cylinder in an aligned magnetic field*," Int. J. Heat Mass Transfer, 47: 4075.

	The first author, **Wilys O. Mukuna BSc(Hons), MSc,** is a lecturer at the Department of Mathematics and Computer Science, University of Kabianga, Kenya and a Doctoral Student at Jomo Kenyatta University of Agriculture and Technology, Kenya.
	The second author, **Jackson K. Kwanza PhD,** Is a Proffessor of Applied Mathematics at the Department of Pure and Applied Mathematics, Jomo Kenyatta University of Agriculture and Technology, Kenya.
	THE third author, **Johana K. Sigey PhD**, is a Professor of Applied Mathematics at the Department of Pure and Applied Mathematics, Jomo Kenyatta University of Agriculture and Technology, Kenya.
	The fourth author, **Jeconiah A. Okelo PhD,** is a Senior Lecturer of Mathematics at the Department of Pure and Applied Mathematics, Jomo Kenyatta University of Agriculture and Technology, Kenya.